High-pressure, high-temperature thermophysical measurements on molybdenum

G Pottlacher, E Kaschnitz and H Jäger

Institut für Experimentalphysik, Technische Universität Graz, Petersgasse 16, 8010 Graz, Austria

Abstract. Wire-shaped molybdenum samples were resistively pulse heated in a coaxial capacitor discharge circuit. Heating rates greater than 10^9 K s^{-1} were attained, and temperatures up to 10 000 K reached. Time-correlated measurements were made with submicrosecond resolution of the current through the wire and voltage drop across it, as well as measurements of surface radiation and wire expansion. These quantities allow determination of such thermophysical properties as the heat capacity at constant pressure and the mutual dependencies between temperature, volume, specific enthalpy and electrical resistivity in superheated liquid molybdenum.

1. Introduction

Pulse heating techniques have been successfully applied to the determination of the thermophysical properties of metals up to temperatures far above the normal boiling point. Using such techniques it is possible to reach regions that are not accessible to static experiments. The heating rates used in this type of experiment vary between 10^4 and 10^9 K s^{-1}.

Such pulse heating techniques are currently employed by several research groups. The following are some of the latest publications by each of these groups.

Millisecond time resolution investigations have been carried out by Müller and Cezairliyan [1] at the National Institute of Standards and Technology in Gaithersburg, Maryland, USA; by Righini et al [2] at the Istituto di Metrologia 'G Colonetti' in Turino, Italy; by Petrova et al [3] at the Institute of High Temperatures, Academy of Sciences of the USSR, Moscow; and by Maglic et al [4] at the Institute for Thermal Engineering and Energy Research, Boris Kidrich Institute of Nuclear Sciences, Beograd, Yugoslavia.

Microsecond time resolution investigations have been carried out by Berthault et al [5] at the Commissariat à l'Energie Atomique in Paris, France; by McClure and Cezairliyan [6] at the National Institute of Standards and Technology in Gaithersburg, Maryland, USA; by Hixson et al [7] at the Los Alamos National Laboratory, New Mexico, USA; and by Scheindlin et al [8] at the Institute of High Temperatures, Academy of Sciences of the USSR, Moscow.

Experiments in the submicrosecond time resolution have been performed by Savvatimskii et al [9] at the Institute of High Temperatures, Academy of Sciences of the USSR, Moscow, and also at our institute.

Our measurements continue the work of Seydel *et al* [10] who established an apparatus with submicrosecond time resolution at the Institut für Experimentalphysik, Universität Kiel, FRG. Our fast discharge circuit is similar to that used by Seydel *et al* [10], and it was improved by Gallob *et al* [11]. Recently we have established a second, slower system, with improved data acquisition and new facilities.

In this work we give the results of some investigations on molybdenum wires using the fast discharge circuit.

2. Experimental details

In our experimental apparatus energy is stored in a 5.4 μF capacitor, with a charging voltage between 4000 and 8000 V. The short circuit ringing period of the circuit is 6.2 μs. For this work the resistivity of the system was 26.3 mΩ and the inductance 180 nH.

The molybdenum wires used in this work were typically 40 mm in length and 0.25 mm in diameter. Goodfellow metals (Cambridge UK) report the purity as 99.99+%. The wire sample was resistively heated with water as the ambient medium to avoid peripheral discharges. The experiment is performed in a high-pressure vessel with sapphire windows and a maximum pressure capability of 0.5 GPa. In this work we used pressures varying from 1 to 2000 bar.
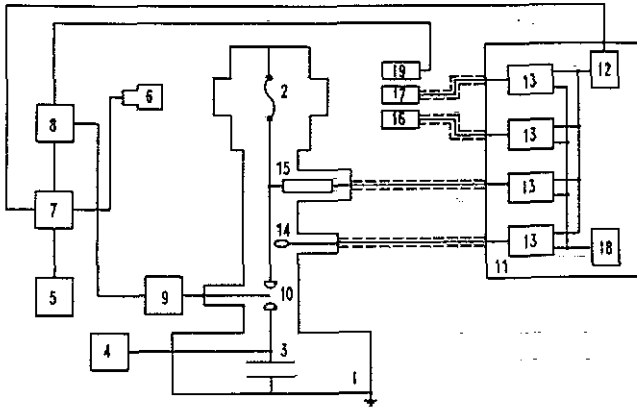

Figure 1. Block diagram of the experimental arrangement: 1, coaxially built-up discharge circuit; 2, wire sample; 3, capacitor bank; 4, charging unit; 5, start pulse; 6, flashlamp; 7, delay; 8, trigger; 9, thyratron; 10, three-electrode spark gap; 11, shielded measuring room; 12, trigger; 13, 200 MHz oscilloscopes; 14, induction coil; 15, voltage divider; 16, pyrometer; 17, photodetector for expansion measurement; 18, time-mark generator; 19, Kerr-cell shutter camera (figure reproduced from [26]).

The principal layout of the experimental setup is shown in figure 1. An initial pulse triggers a flash-light for background illumination and after a delay the main discharge is triggered with the aid of a three-electrode spark gap. At the same time the recording equipment in the screen room is triggered. The quantities measured are:

(i) the current through the wire, measured using an induction coil (the coil signal is subsequently integrated);

(ii) the voltage using a coaxial ohmic voltage divider;

(iii) the surface radiance temperature using a pyrometer with a fast PIN photodiode operating at 800 ± 10 nm (interference filter); and

(iv) the final volume of the sample using a shadowgraph technique employing a camera with a 30 ns exposure time. This camera uses a Kerr-cell shutter.

All measured quantities have rise-times of less than 10 ns. More experimental details are given in [11].

3. Data reduction

Many additional thermophysical properties may be calculated from these measured quantities, and we show schematically how this is done in figure 2.
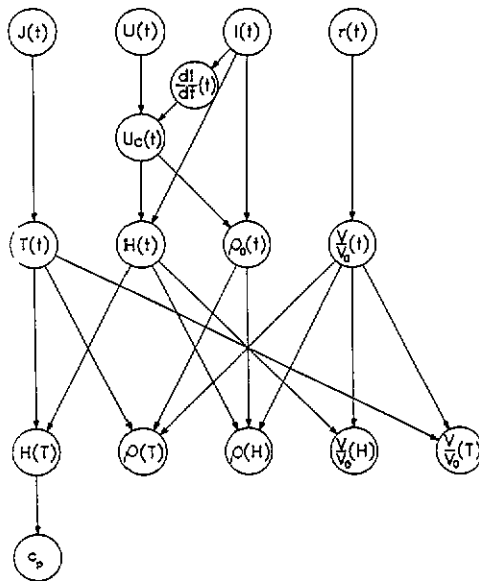

Figure 2. Survey of measured and derived quantities in which t is the time, J the radiation intensity, U the voltage, I the current, r the specimen radius, T the temperature, H the enthalpy, ρ_0 the electric resistivity without taking the volume expansion into consideration, ρ the electric resistivity, V/V_0 the volume change, and C_p the specific heat capacity.

The time-dependent current $I(t)$, voltage $U(t)$ and surface radiation intensity $J(t)$ are measured simultaneously with oscilloscopes. The sample radius $r(t)$ is measured using the previously mentioned shadowgraph technique.

The inductive contributions are subtracted from the measured voltage $U(t)$ to produce the true voltage $U_c(t)$. The specific enthalpy $H(t)$ in MJ kg^{-1}, may be calculated from $U_c(t)$ and $I(t)$, starting at room temperature $[H = H(t) - H(298)]$ from

$$H = \frac{1}{m} \int_0^t I(t) U_c(t) \, dt \qquad (1)$$

where m is the mass of the sample.

The electrical resistivity $\rho_0(t)$ in $\mu\Omega$ m, without a volume correction, can be calculated from

$$\rho_0(t) = \frac{U(t)\pi r_0^2}{I(t)1} \qquad (2)$$

where r_0 is the initial radius in metres and l the length in metres of the specimen.

Measurement of the sample radius $r(t)$ allows determination of the volume change V/V_0 (V_0 is the initial volume). This allows the specific electrical resistivity $\rho(t)$ in $\mu\Omega$ m to be calculated:

$$\rho(t) = \rho_0(t)\frac{r^2(t)}{r_0^2}. \qquad (3)$$

The temperatures are calculated using the known melting temperature of the specimen as the calibration point. Temperatures are found using the Kirchhoff–Planck law, and forming ratios of the radiance at temperature T to the radiance at the melt temperature T_m. This is possible due to the linear amplification of the pyrometer, which has been proved for the whole experimental range. At melt (index m) the pyrometer detects for a certain time (from beginning to end of melt) a constant radiance with the intensity J_m (in volts, at a wavelength of 800 nm):

$$J_m(T_m) = g\epsilon(\lambda, T_m)c_1/\{\lambda^5[\exp(c_2/\lambda T_m) - 1]\}. \qquad (4)$$

Here $J_m(T_m)$ is the measured intensity at the melting point, T_m is the melting temperature, g is a geometric factor, $\epsilon(\lambda, T_m)$ is the spectral emissivity at the melting temperature, c_1 is the first radiation constant, λ is the wavelength in metres and c_2 is the second radiation constant.

At any point in the liquid phase the pyrometer detects an intensity J in volts, at a wavelength of 800 nm:

$$J(T) = g\epsilon(\lambda, T)c_1/\{\lambda^5[\exp(c_2/\lambda T) - 1]\}. \qquad (5)$$

Here $J(T)$ is the measured intensity at the temperature T. The unknown temperature T we obtain from the ratio

$$\frac{J_m(T_m)}{J(T)} \qquad (6)$$

using equations (4) and (5).

$$T = c_2/\lambda \ln\left\{1 + \frac{\epsilon(T)}{\epsilon(T_m)}\frac{J_m(T_m)}{J(T)}[\exp(c_2/\lambda T_m) - 1]\right\}. \qquad (7)$$

For temperatures above the melting point $\epsilon(T)$ was assumed to be constant, i.e. $\epsilon(T) = \epsilon(T_m)$, because of the lack of emissivity data for these states. This assumption means that one does not require emissivity values, as the ratio $[\epsilon(T)/\epsilon(T_m) = 1]$ is assumed to have the value 1. This assumption is typical and has been made by other authors (see e.g. [12]).

These quantities are on the same time base, and by comparing values at common times we find the interdependences of enthalpy, resistivity, temperature and volume expansion, shown in the third row of figure 2.

The slope of the plot of enthalpy against temperature allows the determination of c_p, the specific heat at constant pressure. From the same curve it is also possible to determine the enthalpy of fusion.

Although it is possible with this method to obtain data in the solid region, only values above the onset of melting are given in this work, because more accurate results for the solid phase are available from static measurements. All the figures show the corresponding least-squares fits to our values as well as the least-squares fits to the values from Seydel *et al* [10], and Hixson [13].

4. Results and discussion

The specific enthalpy H is shown in figure 3 as a function of the temperature T for this work. All the results reported here were obtained at a pressure of 2000 bar. The values from Seydel *et al* [10] and Hixson ([13] (who also used a pressure of 2000 bar in argon) are also shown for comparison. As can be seen our results agree well with those of the other two investigations. Our measured values reached temperatures of 10 000 K, which is a region of superheated liquid molybdenum which has not been investigated up to now. The values from static measurements [14, 15] are not indicated in this figure, as they overlap with the values from dynamic measurements and therefore cannot be resolved. The good agreement with these values can be seen from table 1.
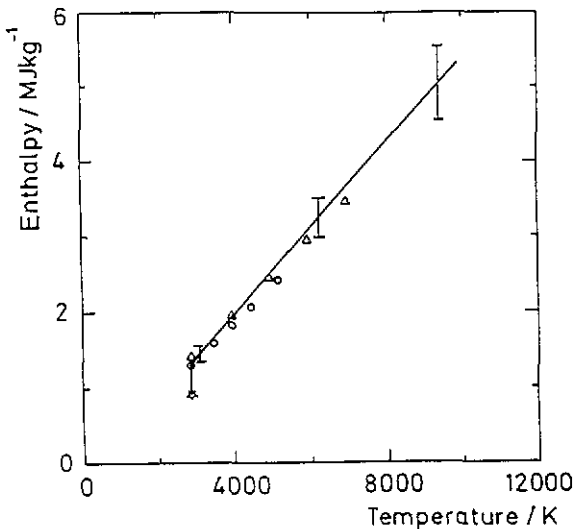

Figure 3. Specific enthalpy H shown as a function of temperature T. The least-squares fit to this work is shown as a full line, with * indicating the start of melting. The values of Seydel *et al* [10] are shown as open triangles, and the values of Hixson [13] are shown as open circles. The pressure is 2000 bar for this figure and all succeeding figures.

The least-squares fit for enthalpy in MJ kg^{-1} to our liquid data in the range $2890 \leq T \leq 10\,000$ K is

$$H = -0.2984 + 5.60 \times 10^{-4} T. \tag{8}$$

The least-squares fits to the values from Seydel *et al* are given in [10] and also in Gathers [16]. The least-squares fit to the values from Hixson will be published in [13].

From the constant radiation at the melting transition in the temperature measurement from figure 3 we find enthalpy values of 0.90 MJ kg^{-1} at the beginning of melt and 1.32 MJ kg^{-1} at the end of melt, leading to a heat of fusion value of 0.42 MJ kg^{-1}.

In table 1 a summary of enthalpy values reported by various authors is given for the beginning and end of the melt, as well as for the heat of fusion. The enthalpy values at the beginning of melt differ by ±4%, at the end of melt by ±5% and for the heat of fusion by ±13% from the values found in this work. This is within our uncertainty estimates.

The derivative of the polynomial (8) gives $c_p = 560$ J kg^{-1} K^{-1} for the specific heat of liquid molybdenum. In table 1 we give a summary of c_p values from other authors, of which all except [14, 15] are obtained by dynamic techniques. The value from Seydel *et al* [10] differs by 10%, the value from Hixson [13] by about 15%, the value from Shaner *et al* [17] by 30%. This value has been corrected by Gathers [21] resulting in a decrease of 14%. This corrected value differs by only 9%, which is the same as the value from Dikther and Lebedev [18]. The recommended value of Desai [14] from static measurements differs by 25%. This wide range in values is due to the fact that c_p depends on temperature measurement, which has the largest error bars of all the measured quantities.

Table 1. Summary of values for the specific enthalpy and the specific electrical resistivity at the melting transition (index s, solid; index L, liquid) and for the specific heat reported by different authors.

Reference	H_s (MJ kg^{-1})	H_L (MJ kg^{-1})	ΔH (MJ kg^{-1})	ρ_s ($\mu\Omega$ m)	ρ_L ($\mu\Omega$ m)	c_p (J kg^{-1} K^{-1})
This work	0.90	1.32	0.42	0.787	0.958	560
Seydel *et al* [10]	0.888	1.393	0.505	0.806	0.971	500
Hixson [13]	0.912	1.29	0.378	0.798	0.958	476
Desai [14, 15]	0.936	1.344	0.408	0.827	—	421
Shaner [17]	0.907	1.28	0.373	0.801	0.955	727
Dikther [18]	—	—	0.42	0.8	0.95	621
Berezin [19]	0.914	1.295	0.381	—	—	—
Cezairliyan [20]	—	—	—	0.797	—	—
Gathers [21]	—	—	—			625

Our measured values of the volume ratio V/V_0 are shown in figure 4 plotted against the enthalpy H. Using a shadowgraph technique [11] we were able to measure the volume expansion from the start of the experiment (room temperature) up to the end of the liquid phase. The values from Seydel *et al* [10] and Hixson [13] are also shown. Hixson's values were also measured at a pressure of 2000 bar and are in good agreement with our values. The volume expansion given by Seydel *et al* [10] seems to have a wrong slope, because at room temperature the ratio V/V_0 must be 1.
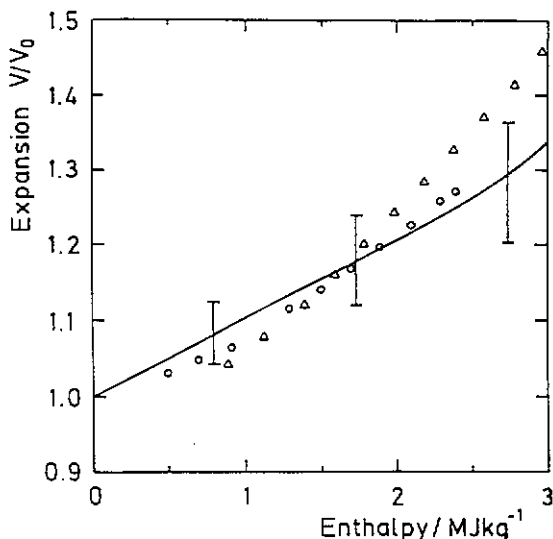
Figure 4. Volume change V/V_0 is plotted against enthalpy H. The least-squares fit to this work is shown as a full line, the open triangles are the values from Seydel *et al* [10], and open circles are the values from Hixson [13].

The corresponding fit to our values for the volume ratio up to 2.40 MJ kg^{-1} is

$$V/V_0 = 1 + 1.03 \times 10^{-1} \, H \tag{9}$$

and in the range $2.40 \leq H \leq 3.60$ MJ kg^{-1}

$$V/V_0 = 1.23 - 1 \times 10^{-1} \, H + 4.47 \times 10^{-2} \, H^2. \tag{10}$$

Ivanov *et al* [22] discussed the problem of optical expansion measurements when water is used as the pressure medium which is what we used. They reached the conclusion that a change occurs in the refractive index of the water which is heated and vaporized near the wire. This process becomes significant at higher temperatures.

In previous investigations [23, 24] we studied the influence of static pressure in the surrounding water on the expansion measurement when using a shadowgraph technique. On the basis of these investigations we can say that at an ambient pressure of 2000 bar, far above the critical point of water, it is certain that there is no significant change in the refractive index of the surrounding water near the surface of the wire which leads to measured volume ratios that are systematically high. Figure 4 shows volume expansions at a pressure of 2000 bar in water that are in good agreement with the values from Hixson [13] with compressed argon gas as ambient medium. The data from Seydel *et al* [10] seem to be taken at a pressure in water of 1 bar, thus leading to volume expansions that are systematically high, as discussed previously. Using an ambient pressure of 1 bar we also found that the volume expansions were too large (Pottlacher *et al* [25]) for example for rhenium.

In figure 5 we present our measured electrical resistivity ρ as a function of enthalpy H along with the values from Seydel *et al* [10] and Hixson [13]. We entirely agree with Hixson's values. The results from Seydel *et al* [10] up to 2.5 MJ kg^{-1} are in the same good agreement with our values; above this value we assume that the resistivity
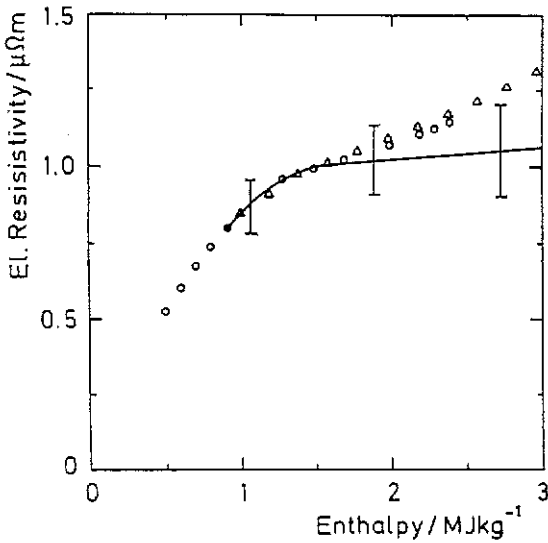
Figure 5. Electrical resistivity ρ is plotted as a function of enthalpy H. The least-squares fit to this work is shown as a full line, the open triangles are the values from Seydel *et al* [10], and the open circles are the values from Hixson [13].

values of Seydel *et al* [10] are influenced by the expansion effect described earlier (equation (3)). This results in resistivity values that are systematically high.

The best fit to our resistivity data ρ in $\mu\Omega$ m for $0.90 \leq H \leq 1.55$ MJ kg^{-1} is given by

$$\rho = 3.65 \times 10^{-8} + 1.12 \times 10^{-6}\, H - 3.23 \times 10^{-7}\, H^2 \tag{11}$$

and for $1.55 \leq H \leq 3.00$ MJ kg^{-1},

$$\rho = 9.42 \times 10^{-7} + 3.93 \times 10^{-8}\, H. \tag{12}$$

In table 1 we gave a summary of the electrical resistivity values at the melting transition reported by different authors. For the beginning of melt we obtain a resistivity value of $0.787\ \mu\Omega$ m. This value is up to 5% less than results from other workers. For the end of melt we obtain a resistivity value of $0.958\ \mu\Omega$ m, and values obtained by other workers do not deviate by more than 2% from this.

The best fit to relative volume change V/V_0 is shown in figure 6 plotted against temperature T (drawn as a full line for this work). Since our pyrometer at this time was not sensitive to temperatures below 2500 K, our data start with the onset of melting. The values from Seydel *et al* [10] and Hixson [13], who obtained data for the solid phase as well as the liquid phase, are also shown. Our results agree quite well with Hixson's for the liquid. The volume expansion values given by Seydel *et al* [10], on the other hand, are somewhat higher.

For convenience and practical use figure 7 presents the electrical resistivity plotted as a function of temperature T. For both figures 5 and 6 no least-squares fits were calculated, as the data can be derived from equations (8)–(12). The values from Seydel *et al* [10] and Hixson [13] are again shown. Our resistivity values for temperatures above 4000 K lie somewhat lower than those given by Seydel *et al* [10] and Hixson, but
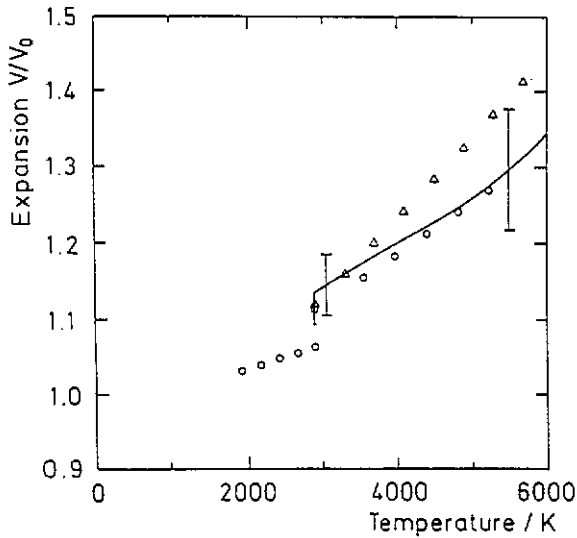
Figure 6. Volume change V/V_0 is plotted against temperature T. The measured values from this work are shown as a full line, the open triangles are the values from Seydel *et al* [10], and the open circles are the values from Hixson [13].
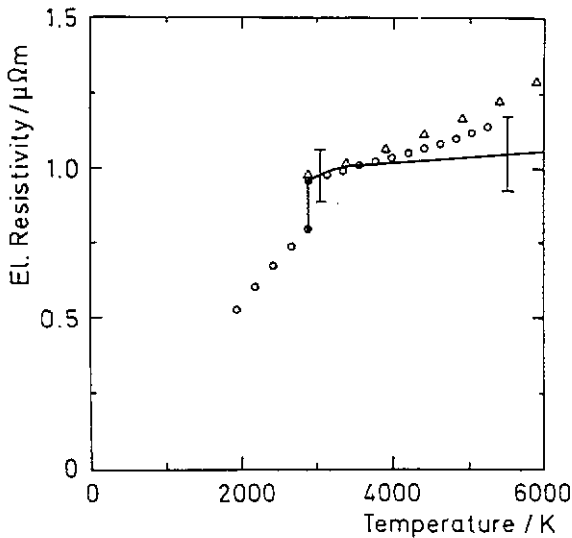

Figure 7. Electrical resistivity ρ is shown as a function of temperature T. The measured values of this work are the full line, the open triangles are the values from Seydel *et al* [10], and the open circles are the values from Hixson [13].

agree with those of Hixson within our error bars. Our resistivity values, for example, for tungsten were also less than those found by other workers (Kaschnitz *et al* [26]). One reason for this trend might be the high purity of the samples we used, purities which may not have been available ten years ago. The trend to lower values may also be seen from the values from Hixson [13].

5. Estimation of errors

For pulse heating experiments, reliable estimates of the total experimental uncertainty are difficult to make. Error bars associated with each measured thermophysical quantity are shown in the figures for points at the beginning, in the middle, and at the end of the experimental range investigated. All obtained data fall within those uncertainty estimates. An error of 5% is to be assumed for the enthalpy, and 9% for the electrical resistivity close to the melting transition, increasing to about 13% at the upper end of our experimental range. The uncertainty in the temperature measurement does not exceed 10%. The uncertainty of the specific heat for liquid molybdenum therefore should not exceed 15%. A detailed discussion of experimental difficulties and of sources of errors for such kind of pulse heating experiments has been given by Cezairliyan [27].

References

[1]   Müller A P and Cezairliyan A 1990 *Int. J. Thermophys.* **11** 619
[2]   Righini F, Bussolino G C, Rosso A and Roberts R B 1990 *Int. J. Thermophys.* **11** 629
[3]   Petrova I I and Ya Chekhovskii V 1988 *High Temp.* **26** 198
[4]   Dobrosavljevic A S, Maglic K D and Perovic N L 1989 *High Temp. High Press.* **21** 317
[5]   Berthault A, Arles L and Matricon J 1986 *Int. J. Thermophys.* **7** 167
[6]   McClure J L and Cezairliyan A 1990 *Int. J. Thermophys.* **11** 739
[7]   Hixson R S and Winkler M A 1990 *High Press. Res.* **4** 555
[8]   Sheindlin M A and Senchenko V N 1987 *High Temp.* **25** 281
[9]   Lebedev S V and Savvatimskii U I 1984 *Sov. Phys. Usp.* **27** 749
[10] Seydel U, Fucke W and Wadle H 1980 *Die Bestimmung thermophysikalischer Daten flüssiger hochschmelzender Metalle mit schnellen Pulsaufheizexperimenten* (Düsseldorf: P. Mannhold)
[11] Gallob R, Jäger H and Pottlacher G 1986 *Int. J. Thermophys.* **7** 139
[12] Gathers G R, Shaner J W and Brier R L 1976 *Rev. Sci. Instrum.* **47** 471
[13] Hixson R S 1991 *Int. J. Thermophys.* at press
[14] Desai P D 1987 *J. Phys. Chem. Ref. Data* **16** 91
[15] Desai P D, Chu T K, James H M and Ho C Y 1984 *J. Phys. Chem. Ref. Data* **13** 1069
[16] Gathers G R 1986 *Rep. Prog. Phys.* **49** 342
[17] Shaner J W, Gathers G R and Minichino C 1977 *High Temp. High Press.* **9** 331
[18] Dikhter I Ya and Lebedev S V 1972 *High Temp.* **9** 845
[19] Berezin B Ya, Chekhovskoi V Ya and Scheindlin A E 1971 *High Temp. High Press.* **3** 287
[20] Cezairliyan A, Morse M S and Beckett C W 1970 *Rev. Int. Hautes Temper. et Refract.* **7** 382
[21] Gathers G R 1983 *Int. J. Thermophys.* **4** 149
[22] Ivanov V V, Lebedev S V and Savvatimskii A I 1984 *J. Phys. F: Met. Phys.* **14** 1641
[23] Kaschnitz E 1988 *Diplomarbeit* Technische Universität Graz
[24] Jäger H, Neff W and Pottlacher G 1992 *Proc. Second Workshop on Subsecond Thermophysics, (Turin, Italy 1990), Int. J. Thermophys.* at press
[25] Pottlacher G, Neger T and Jäger H 1986 *Int. J. Thermophys.* **7** 149
[26] Kaschnitz E, Pottlacher G and Windholz L 1990 *High Press. Res.* **4** 558
[27] Cezairliyan A 1984 *Compendium of Thermophysical Property Measurements Methods* vol 1, ch 16, ed K D Maglic, A Cezairliyan and V E Peletsky (New York: Plenum)